Astrodynamics Vol. 8, No. 1, 135–148, 2024 https://doi.org/10.1007/s42064-023-0183-3

Characterization of Gauss–Markov stochastic sequences for mission analysis

Carmine Giordano (✉)

Department of Aerospace Science and Technology, Politecnico di Milano, Milano 20156, Italy

ABSTRACT

In real scenarios, the spacecraft deviates from the intended paths owing to uncertainties in dynamics, navigation, and command actuation. Accurately quantifying these uncertainties is crucial for assessing the observability, collision risks, and mission viability. This issue is further magnified for CubeSats because they have limited control authority and thus require accurate dispersion estimates to avoid rejecting viable trajectories or selecting unviable ones. Trajectory uncertainties arise from random variables (e.g., measurement errors and drag coefficients) and processes (e.g., solar radiation pressure and low-thrust acceleration). Although random variables generally present minimal computational complexity, handling stochastic processes can be challenging because of their noisy dynamics. Nonetheless, accurately modeling these processes is essential, as they significantly influence the uncertain propagation of space trajectories, and an inadequate representation can result in either underestimation or overestimation of the stochastic characteristics associated with a given trajectory. This study addresses the gap in characterizing process uncertainties, represented as Gauss–Markov processes in mission analysis, by presenting models, evaluating derived quantities, and providing results on the impact of spacecraft trajectories. This study emphasizes the importance of accurately modeling random processes to properly characterize stochastic spacecraft paths.

KEYWORDS

Gauss–Markov process
uncertainty quantification
stochastic dynamics
Monte Carlo simulation

Research Article

Received: 30 May 2023
Accepted: 14 September 2023

1 Introduction

In a real-life scenario, a spacecraft is unlikely to follow the prescribed nominal path owing to uncertainties in *dynamics* (e.g., gravitational parameters or noisy radiation pressure profiles), *navigation* (i.e., imperfect state knowledge or approximations in the measurement model), and *command actuation* (i.e., thrust magnitude and pointing angle error) [1]. The correct quantification of these uncertainties and their impact on the spacecraft trajectory is a required task in space operations, for example, to evaluate the observability of a spacecraft trajectory or assess the collision risk with another object [2]. In mission analysis, uncertainty quantification is of paramount importance for determining the flyability of trajectories, and consequently, the feasibility of spacecraft missions. In fact, it is not uncommon that even if they can be nominally exploited, some trajectories are not useful after an uncertainty assessment is performed owing to navigation costs [3] or risks [4].

Uncertainties related to spacecraft trajectory analysis are random variables (e.g., measurement errors, drag coefficients, and mass parameters, which are usually modeled as Gaussian variables) and random processes (e.g., solar radiation pressure and low thrust acceleration). Although random variables usually do not pose any additional complexity from a computational perspective, stochastic processes can be difficult to handle because of their noisy dynamics. Nevertheless, their impact on propagation under space trajectory uncertainty is relevant, and improper modeling can lead to under- or overestimation of the stochastic characteristics of the

✉ carmine.giordano@polimi.it

given trajectory. Particularly, errors in the estimation of the dispersion, i.e., the distance between the real and nominal trajectory, can lead to the discarding of feasible trajectories (in the case of over-estimation) or to the selection of unflyable trajectories, requiring a large amount of propellant when in flight (in the case of under-estimation). Therefore, the characterization of random processes, usually represented as Gauss–Markov processes in mission analysis tasks, their modeling as discrete processes to be used inside a computational algorithm, and the assessment of their impact on uncertain propagation are critical.

In mission analysis, Gauss–Markov processes are commonly used in navigation tasks in a linearized sense [5, 6], and models exist for certain nonlinear uncertainty propagation algorithms [7]. However, the impact of computational-compliant discrete models of Gauss–Markov processes on spacecraft trajectories remains incomplete in the context of Monte Carlo simulations, essential for dispersion analysis, as well as the characterization of their derived quantities.

The remainder of this paper is structured as follows. Section 2 presents the Gauss–Markov processes and their properties. The driving noise characteristics together with two discrete models for the processes are presented in Section 3, and Section 4 presents an assessment of some derived quantities of interest in the mission analysis. The results are presented in Section 5 and the conclusions are given in Section 6.

2 Gauss–Markov processes

In spacecraft trajectory design, stochastic processes are usually regarded as stationary Gauss–Markov processes, also known as Ornstein–Uhlenbeck processes [5]. These are random functions whose characteristics do not change when shifted in time and enjoy both Gaussian and Markov properties, that is, every variable subset has a multivariate normal distribution, and every variable transition probability depends only on the immediately preceding state and not on the full past history [8]. Generally, a Gauss–Markov process $\eta(t)$ follows the Langevin differential equation in a heuristic manner [9]:

$$\dot{\eta}(t) = -\beta\eta(t) + \omega(t) \tag{1}$$

where ω is the noise with zero mean and finite variance σ_ω, and $\beta = 1/\tau$ is the inverse of the correlation time τ. Equation (1) is a first-order linear ordinary differential equation and its solution is [5, 10]:

$$\eta(t) = \eta_0 \mathrm{e}^{-\beta(t-t_0)} + \int_{t_0}^{t} \mathrm{e}^{-\beta(t-\tau)}\omega(\tau)\mathrm{d}\tau \tag{2}$$

with $\eta_0 = \eta(t_0)$. Because the integral part is a function of the noise, Eq. (2) cannot be computed analytically, but can be evaluated only in a stochastic sense. Since $E[\omega] = 0$ by definition, the stochastic integral has a null mean. Thus,

$$\bar{\eta} = E[\eta(t)] = \eta_0 \mathrm{e}^{-\beta(t-t_0)} \tag{3}$$

The process mean depends only on the value of the initial distribution, and vanishes exponentially over time. If a nonzero-mean process is required, the Vasicek model can be exploited [11]. The associated Langevin equation is expressed as Eq. (4):

$$\dot{\eta}(t) = -\beta(\eta(t) - \mu) + \omega(t) \tag{4}$$

where μ is a constant that represents the steady-state mean. In fact, the general solutions to Eq. (4) are as Eq. (5):

$$\eta(t) = \mu + (\eta_0 - \mu)\mathrm{e}^{-\beta(t-t_0)} + \int_{t_0}^{t} \mathrm{e}^{-\beta(t-\tau)}\omega(\tau)\mathrm{d}\tau \tag{5}$$

and

$$\lim_{t\to\infty} \eta(t) = \mu \tag{6}$$

In this study, only the unbiased Gaussian–Markov process was considered, without loss of generality.

The autocorrelation function for a general Gaussian–Markov process between two generic time t_1 and t_2 is evaluated as [12]:

$$R_\eta(t_1, t_2) = E[\eta(t_1)\eta(t_2)] = \mathrm{e}^{-\beta(t_2-t_1)} R_\eta(t_1) \tag{7}$$

where $R_\eta(t_1)$ is the autocorrelation of η at time t_1:

$$\begin{aligned} R_\eta(t_1) &= E[\eta(t_1)\eta(t_1)] \\ &= \sigma_{\eta_0}^2 \mathrm{e}^{-2\beta(t_1-t_0)} + \frac{\sigma_\omega^2}{2\beta}\left(1 - \mathrm{e}^{-2\beta(t_1-t_0)}\right) \end{aligned} \tag{8}$$

One of the most important characteristics of Gauss–Markov processes can be inferred from Eq. (7), which decreases exponentially with time at a rate that depends on the correlation time τ. Therefore, the values drawn from this type of stochastic process are also known as exponentially correlated random variables (ECRV).

3 Driving noise characterization

3.1 Continuous driving noise

The stochastic characteristics of Gauss–Markov processes are functions of the driving noise. However, in

astrodynamic applications, noise statistics are not easily available, and the process characteristics can be inferred directly from experimental or historical data. Thus, to correctly model Gauss–Markov processes in numerical simulations, it is crucial to evaluate the driving noise covariance starting from the process values.

The Gauss–Markov variance can be derived directly from Eq. (8). In fact, for a generic time t,

$$\begin{aligned}\sigma^2 &= E[(\eta(t)-\bar{\eta})(\eta(t)-\bar{\eta})] = E[\eta(t)\eta(t)] - \bar{\eta}^2 \\ &= \sigma_{\eta_0}^2 \mathrm{e}^{-2\beta(t-t_0)} + \frac{\sigma_\omega^2}{2\beta}\left(1-\mathrm{e}^{-2\beta(t-t_0)}\right) - \bar{\eta}_0^2 \mathrm{e}^{-2\beta(t-t_0)}\end{aligned} \tag{9}$$

where $\sigma_{\eta_0}^2 = E[\eta_0^2]$. Without loss of generality, the initial process can be drawn from a normal distribution with a zero mean and a prescribed standard deviation σ, that is, $\eta_0 \sim \mathcal{N}(0, \sigma^2)$. In this case, the noise standard deviation σ_ω can be directly inferred from the process variance, as Eq. (10):

$$\sigma_\omega = \sqrt{2\beta}\sigma \tag{10}$$

It is noteworthy that Eq. (9) is singular when computing σ_ω for $t = t_0$. However, because $\sigma = \sigma_{\eta_0}$ at t_0 for any choice of σ_ω, Eq. (10) can be extended to $t = t_0$.

3.2 Discrete driving sequence

The use of Gaussian driving noise is impractical in the case of numerical simulations of a system depending on Gauss–Markov process because integration schemes cannot cope with continuous noise and will generally fail. Therefore, in practical applications, white noise is usually substituted with a random driving sequence, that is, a piecewise constant function $\omega(t) = \hat{\omega}(t)$ with a constant value ω_k when $t \in [t_k, t_{k+1}]$. In this case, the Langevin equation can be numerically solved using integration schemes for stochastic differential equations (SDE), such as the Euler–Maruyama scheme, Milstein method, and the SDE Runge–Kutta scheme [13]. For example, the Euler–Maruyama scheme is an extension of the forward Euler method, which integrates the SDE. In the case of a Gauss–Markov process, the forward step is defined as

$$\eta_{k+1} = \eta_k - \beta\eta_k\delta t + \omega_k\sqrt{\delta t} \tag{11}$$

where the subscripts correlate with time and $\delta t = t_{k+1} - t_k$. The second term in Eq. (11) represents the forward Euler step of the deterministic part. The last term can be interpreted as the forward step for the nominal Gaussian random sequence, with the standard deviation divided by $\sqrt{\delta t}$.

However, trajectories are usually computed by integrating the spacecraft dynamics using high-order variable-step solvers. This choice allows for accurate solutions with a reasonable computational effort. However, traditional SDE solvers cannot operate with variable-step schemes because they depend on the step itself. Therefore, an alternative modelization that can be used in the traditional variable-step methods is required. Moreover, the model can provide a Gauss–Markov process solution at any time, as required by the integration scheme.

3.2.1 *Solution-preserving model*

In the case of a random sequence, the solution can be split into $n = \left\lceil \frac{t-t_0}{t_{k+1}-t_k} \right\rceil$ time domains, each with a constant driving noise. For each time domain, Eq. (2) can be applied as

$$\begin{aligned}\eta_{k+1} &= \eta_k \mathrm{e}^{-\beta(t_{k+1}-t_k)} + \int_{t_k}^{t_{k+1}} \mathrm{e}^{-\beta(t_{k+1}-\tau)}\omega_k \mathrm{d}\tau \\ &= \eta_k \mathrm{e}^{-\beta(t_{k+1}-t_k)} + \frac{\omega_k}{\beta}\left(1-\mathrm{e}^{-\beta(t_{k+1}-t_k)}\right)\end{aligned} \tag{12}$$

where a constant value of ω_k is used. Combining Eq. (12) for all subintervals from t_0 to $t_n \leqslant t \leqslant t_{n+1}$, a general solution can be obtained, which is

$$\begin{aligned}\eta(t) = {} & \eta_0 \mathrm{e}^{-n\beta\delta t}\mathrm{e}^{-\beta(t-t_n)} \\ & + \frac{1}{\beta}\sum_{k=0}^{n-1}\left[\omega_k\left(1-\mathrm{e}^{-\beta\delta t}\right)\mathrm{e}^{-\beta(t-t_{k+1})}\right] \\ & + \frac{\omega_n}{\beta}\left(1-\mathrm{e}^{-\beta(t-t_n)}\right)\end{aligned} \tag{13}$$

where $\delta t = t_{k+1} - t_k$ denotes the random sequence characteristic.

Moreover, from Eq. (13), a more precise formula linking noise and process variance can be obtained by exploiting the analytical solution of a Gauss–Markov process subjected to a driving random sequence. Indeed,

$$\begin{aligned}\sigma^2 = {} & E\left[\eta_0^2 \mathrm{e}^{-2n\beta\delta t}\mathrm{e}^{-2\beta(t-t_n)}\right] \\ & + \frac{1}{\beta^2}E\left[\left\{\sum_{k=0}^{n-1}\left[\omega_k\left(1-\mathrm{e}^{-\beta\delta t}\right)\mathrm{e}^{-\beta(t-t_{k+1})}\right]\right. \right. \\ & \left. \left. + \frac{\omega_n}{\beta}\left(1-\mathrm{e}^{-\beta(t-t_n)}\right)\right\}^2\right]\end{aligned} \tag{14}$$

where the independence of the random sequence and the initial process distribution were exploited. Because $E[\omega_k\omega_n] = \sigma_\omega^2\delta(t_k - t_n)$ by definition, where δ is the Dirac delta function, Eq. (14) can be simplified as Eq. (15):

$$\sigma^2 = \sigma_{\eta_0}^2 \mathrm{e}^{-2n\beta\delta t}\mathrm{e}^{-2\beta(t-t_n)} + \frac{1}{\beta^2}E\left[\left[\sum_{k=0}^{n-1}\omega_k\left(1-\mathrm{e}^{-\beta\delta t}\right)\mathrm{e}^{-\beta(t-t_{k+1})}\right]^2 + \left[\omega_n\left(1-\mathrm{e}^{-\beta(t-t_n)}\right)\right]^2\right] = \sigma_{\eta_0}^2 \mathrm{e}^{-2n\beta\delta t}\mathrm{e}^{-2\beta(t-t_n)} + \frac{1}{\beta^2}\left(1-\mathrm{e}^{-\beta\delta t}\right)^2\mathrm{e}^{-2\beta(t-t_n)} \cdot E\left[\sum_{k=0}^{n-1}\left(\omega_k\mathrm{e}^{-\beta(n-k-1)\delta t}\right)^2\right] + \frac{1}{\beta^2}\left(1-\mathrm{e}^{-\beta(t-t_n)}\right)^2 E[\omega_n^2] \tag{15}$$

where the property $E[\omega_k\omega_h] = \sigma_\omega^2\delta(t_k - t_h)$ is exploited again, considering that $t - t_{k+1} = t - t_n + (n-k-1)\delta t$. Considering the summation as a geometric series, the previous expression can be simplified as Eq. (16):

$$\sigma^2 = \sigma_{\eta_0}^2 \mathrm{e}^{-2n\beta\delta t}\mathrm{e}^{-2\beta(t-t_n)} + \frac{1}{\beta^2}\left(1-\mathrm{e}^{-\beta\delta t}\right)^2 \cdot \mathrm{e}^{-2\beta(t-t_n)}\left(1-\frac{1-\mathrm{e}^{-2\beta(n-1)\delta t}}{1-\mathrm{e}^{2\beta\delta t}}\right)\sigma_\omega^2 + \frac{1}{\beta^2}\left(1-\mathrm{e}^{-\beta(t-t_n)}\right)^2\sigma_\omega^2 \tag{16}$$

After mathematical manipulation, considering $\sigma_{\eta_0} = \sigma$, the expression in Eq. (16) is rearranged as Eq. (17):

$$\left(1-\mathrm{e}^{-2\beta(t-t_0)}\right)\sigma^2 = \frac{1}{\beta^2}\left[\left(1-\mathrm{e}^{-\beta(t-t_n)}\right)^2 + \chi\mathrm{e}^{-2\beta(t-t_n)}\right]\sigma_\omega^2 \tag{17}$$

where $\chi = (1-\mathrm{e}^{-2\beta n\delta t})\tanh(\beta\delta t/2)$. Hence, the standard driving noise variation is

$$\sigma_\omega = \beta\sqrt{\frac{1-\mathrm{e}^{-2\beta(t-t_0)}}{\left(1-\mathrm{e}^{-\beta(t-t_n)}\right)^2 + \chi\mathrm{e}^{-2\beta(t-t_n)}}}\sigma \tag{18}$$

Usually, the random sequence characteristic time is smaller than the correlation time, that is, $(t-t_n) \leqslant \delta t \ll \tau = 1/\beta$, representing the integration over time of the constant noise of variance σ. In this case, $\mathrm{e}^{-\beta(t-t_n)} \to 1$ and $\tanh(\beta\delta t/2) \to \beta\delta t/2$. Thus, Eq. (18) is simplified to

$$\sigma_\omega = \sqrt{\frac{2\beta}{\delta t}}\sigma \tag{19}$$

As expected, in this case, the driving sequence variance is modified with the sequence characteristic time δt, as in the Euler–Maruyama scheme, because the solution-preserving model can be considered a continuous extension of that model. Moreover, it can be noted that a small δt can increase the fidelity of the model; however, it can lead to an unbearable computational burden and a huge value for the noise variance.

3.2.2 Statistics-preserving model

Alternatively, Eq. (2) represents a Gaussian process that is uniquely defined by its mean and covariance. Hence, to obtain a discrete process that is equivalent to the original continuous process, the integral part of Eq. (2) can be substituted with a function with a zero mean and variance equal to Eq. (9). In this last case, one of the possible alternatives could be [5]:

$$\eta_{k+1} = \eta_k\mathrm{e}^{-\beta(t_{k+1}-t_k)} + \omega_k\sqrt{\frac{1}{2\beta}\left(1-\mathrm{e}^{-2\beta(t_{k+1}-t_k)}\right)} \tag{20}$$

The general solution for the Gauss–Markov discrete process in this case is

$$\eta(t) = \eta_0\mathrm{e}^{-n\beta\delta t}\mathrm{e}^{-\beta(t-t_n)} + \sum_{k=0}^{n-1}\left[\omega_k\sqrt{\frac{1}{2\beta}\left(1-\mathrm{e}^{-2\beta\delta t}\right)}\mathrm{e}^{-\beta(t-t_{k+1})}\right] + \omega_n\sqrt{\frac{1}{2\beta}\left(1-\mathrm{e}^{-2\beta(t-t_n)}\right)} \tag{21}$$

and its variance, reported back to the general solution, can be computed as

$$\sigma^2 = \sigma_{\eta_0}^2\mathrm{e}^{-2n\beta\delta t}\mathrm{e}^{-2\beta(t-t_n)} + \frac{1}{2\beta}\left(1-\mathrm{e}^{-2\beta n\delta t}\mathrm{e}^{-2\beta(t-t_n)}\right)\sigma_\omega^2 \tag{22}$$

Assuming $\sigma_{\eta_0} = \sigma$ and because $t - t_n + n\delta t = t - t_0$, the standard deviation of the driving noise can be inferred as Eq. (23):

$$\sigma_\omega = \sqrt{2\beta}\,\sigma \tag{23}$$

As expected, the statistics-preserving model sequence mimics the continuous model noise as per its design.

Even though Eq. (18) and Eq. (23) provide two different formulas for the driving noise variance, they can be used equivalently because they simply descend from two different models of the same underlying phenomenon. The first model preserves the solution structure but requires a tweak in the driving noise standard deviation to obtain the correct process statistics, whereas the second model preserves the stochastic characteristics but requires a modification of the process solution. Following Eqs. (19) and (23), the link between the two models is represented by the square root of the sequence characteristic time $\sqrt{\delta t}$.

4 Derived quantity characterization

Quantities derived from the Gauss–Markov process are also of interest in trajectory design. Thus, it is crucial

to evaluate the compatibility between computational-compliant models and derived continuous quantities. Additionally, if feasible, establishing a direct connection between the statistics of the derived quantities and the characteristics of the generated Gauss–Markov process through a closed formula holds great significance. This approach can potentially save time and resources by circumventing the need for lengthy and useless simulations.

By exploiting the properties of the mean and covariance, it is straightforward to determine the characteristics of the quantity of interest in the case of a linear combination. For a generic variable $q = a\eta(t) + b$,

$$E[q] = \bar{q} = a\bar{\eta} + b \tag{24}$$

$$E[(q - \bar{q})^2] = a^2\sigma^2 \tag{25}$$

Exploiting this, it is possible to generate a "standard" Gauss–Markov process with a null mean and unitary standard deviation and, later, to shift and scale it to the desired values as a usual Gaussian variable. Thus, if a Gauss–Markov process with a mean μ and standard deviation σ must be generated, it can be performed by defining the quantity:

$$\eta(t) = \sigma\nu(t) + \mu \tag{26}$$

where $\nu(t)$ is the standard process; thus, $\sigma_\omega = \sqrt{2\beta}$. It can be proven that the process in Eq. (26) has exponential time correlation [14].

4.1 Gauss–Markov process integral

The integral of the Gauss–Markov processes in time is found when a condensed measure is used instead of an instantaneous one. For example, Δv can be computed as the time integral of thrust during the entire maneuver. Moreover, in this case, engine manufacturers provide only thrust statistics. Thus, if an impulsive-maneuvers approach is used in the trajectory design, it is necessary to retrieve the statistics on Δv starting from the data on the thruster. The computation of Δv statistics is used as an example of the Gauss–Markov process integral case.

In general, the thrust magnitude process can be expressed using Eq. (26), as shown in Eq. (27):

$$T(t) = \sigma\nu(t) + \overline{T} \tag{27}$$

where σ is the prescribed process standard deviation, and $\overline{T}$ is the thrust mean.

Under these assumptions, Δv can be computed as

$$\Delta v = \int_{t_0}^{t_\mathrm{f}} \frac{T(t)}{m}\mathrm{d}t = \int_{t_0}^{t_\mathrm{f}} \frac{\sigma\nu(t) + \overline{T}}{m}\mathrm{d}t \tag{28}$$

Assuming that the mass is constant, and defining $\Delta t = t_\mathrm{f} - t_0$, the integral is

$$\Delta v = \frac{\sigma}{m}\int_{t_0}^{t_\mathrm{f}} \nu(t)\mathrm{d}t + \frac{\overline{T}}{m}\Delta t \tag{29}$$

4.1.1 Continuous driving noise

Under the assumption of a (theoretically) continuous driving noise, the standard process solution is given by Eq. (2). Thus, Eq. (29) becomes

$$\Delta v = \frac{\sigma}{m}\left(\int_{t_0}^{t_\mathrm{f}} \nu_0 \mathrm{e}^{-\beta(t-t_0)}\mathrm{d}t + \int_{t_0}^{t_\mathrm{f}}\int_{t_0}^{t} \mathrm{e}^{-\beta(t-\tau)}\omega(\tau)\mathrm{d}\tau\mathrm{d}t\right) + \frac{\overline{T}}{m}\Delta t \tag{30}$$

Because $\nu(t)$ has a null mean by definition, the integral part of Eq. (29) has a null mean. Thus,

$$\overline{\Delta v} = E[\Delta v] = \frac{\overline{T}}{m}\Delta t \tag{31}$$

The variance can be computed as

$$\begin{aligned}\sigma^2_{\Delta v} &= E\left[(\Delta v - \overline{\Delta v})^2\right] \\ &= \frac{\sigma^2}{m^2}\left(E\left[\int_{t_0}^{t_\mathrm{f}} \nu_0 \mathrm{e}^{-\beta(t-t_0)}\mathrm{d}t \int_{t_0}^{t_\mathrm{f}} \nu_0 \mathrm{e}^{-\beta(r-t_0)}\mathrm{d}r\right]\right. \\ &\quad + E\left[\int_{t_0}^{t_\mathrm{f}}\int_{t_0}^{t} \mathrm{e}^{-\beta(t-\tau)}\omega(\tau)\mathrm{d}\tau\mathrm{d}t\right. \\ &\quad \left.\left.\cdot \int_{t_0}^{t_\mathrm{f}}\int_{t_0}^{r} \mathrm{e}^{-\beta(r-\rho)}\omega(\rho)\mathrm{d}\rho\mathrm{d}r\right]\right)\end{aligned} \tag{32}$$

where the independence of ν_0 from noise was considered. By exploiting the properties of the expected value and integral operator, it can be conveniently written as

$$\begin{aligned}\sigma^2_{\Delta v} &= \frac{\sigma^2}{m^2}\left(E\left[\nu_0^2\right]\int_{t_0}^{t_\mathrm{f}} \mathrm{e}^{-\beta(t-t_0)}\mathrm{d}t \int_{t_0}^{t_\mathrm{f}} \mathrm{e}^{-\beta(r-t_0)}\mathrm{d}r\right. \\ &\quad + \int_{t_0}^{t_\mathrm{f}}\int_{t_0}^{t_\mathrm{f}}\int_{t_0}^{t}\int_{t_0}^{r} \mathrm{e}^{-\beta(t-\tau)}\mathrm{e}^{-\beta(r-\rho)} \\ &\quad \left.\cdot E\left[\omega(\tau)\omega(\rho)\right]\mathrm{d}\rho\mathrm{d}\tau\mathrm{d}r\mathrm{d}t\right) \\ &= \frac{\sigma^2}{m^2}\left[\frac{1}{\beta^2}(1 - \mathrm{e}^{-\beta\Delta t})^2 + \int_{t_0}^{t_\mathrm{f}}\int_{t_0}^{t_\mathrm{f}}\int_{t_0}^{t}\int_{t_0}^{r} \mathrm{e}^{-\beta(t-\tau)}\right. \\ &\quad \left.\cdot \mathrm{e}^{-\beta(r-\rho)}\sigma_\omega^2\delta(\tau-\rho)\mathrm{d}\rho\mathrm{d}\tau\mathrm{d}r\mathrm{d}t\right] \\ &= \frac{\sigma^2}{m^2}\left[\frac{1}{\beta^2}(1 - \mathrm{e}^{-\beta\Delta t})^2\right. \\ &\quad \left. + \frac{\sigma_\omega^2}{\beta^2}\left(\Delta t + \frac{4\mathrm{e}^{-\beta\Delta t} - \mathrm{e}^{-2\beta\Delta t} - 3}{2\beta}\right)\right]\end{aligned} \tag{33}$$

where δ is Dirac's delta and $E\left[\nu_0^2\right]=1$ by definition.

Given that $\sigma_\omega=\sqrt{2\beta}$, Eq. (33) can be further simplified as

$$\sigma_{\Delta v}^2=\frac{\sigma^2}{m^2}\frac{2}{\beta}\left(\Delta t-\frac{1-\mathrm{e}^{-\beta\Delta t}}{\beta}\right) \tag{34}$$

Assuming that the maneuver duration is well below the autocorrelation time, that is, $\tau=1/\beta\gg\Delta t$ (or, alternatively, $\beta\Delta t\approx 0$), $1-\mathrm{e}^{-\beta\Delta t}\approx 1-\beta\Delta t+\beta^2\Delta t^2/2$, and Eq. (34) can be simplified as

$$\sigma_{\Delta v}^2=\frac{\sigma^2}{m^2}\Delta t^2 \tag{35}$$

4.1.2 Discrete driving sequence

To obtain a computationally compliant algorithm, the noise should be modeled as a random sequence. Because there is no interest in the instantaneous solution itself, the statistics-preserving model, as in Section 3.2.2, is the most suitable model. In this case, the solution can be split into $n=\left\lfloor\frac{t-t_0}{t_{k+1}-t_k}\right\rfloor$ time domains. By substituting the solution into Eqs. (20) and (29) and splitting the time domain, we obtain

$$\begin{aligned}
&\int_{t_0}^{t_\mathrm{f}}\nu(t)\mathrm{d}t\\
&=\sum_{k=0}^{n-1}\int_{t_k}^{t_{k+1}}\left[\nu_k\mathrm{e}^{-\beta(t-t_k)}+\sqrt{\frac{1}{2\beta}\left(1-\mathrm{e}^{-2\beta(t-t_k)}\right)}\omega_k\right]\mathrm{d}t\\
&=\frac{1}{\beta}\sum_{k=0}^{n-1}\Bigg[\underbrace{\left(1-\mathrm{e}^{-\beta\delta t}\right)}_{\alpha}\nu_k\\
&\quad+\underbrace{\frac{1}{\sqrt{2\beta}}\left(\operatorname{arcoth}\left(\frac{\mathrm{e}^{\beta\delta t}}{\sqrt{\mathrm{e}^{2\beta\delta t}-1}}\right)-\sqrt{1-\mathrm{e}^{-2\beta\delta t}}\right)}_{\gamma}\omega_k\Bigg]
\end{aligned} \tag{36}$$

with $\delta t=t_{k+1}-t_k$. It should be noted that both coefficients α and γ are constants and do not depend on the sum index. Hence, the impulse can be computed as

$$\Delta v=\frac{\sigma}{m\beta}\sum_{k=0}^{n-1}(\alpha\nu_k+\gamma\omega_k)+\frac{\bar{T}}{m}\Delta t \tag{37}$$

The stochastic characteristics of Δv can be computed using Eq. (37). The mean is

$$\overline{\Delta v}=E\left[\Delta v\right]=\frac{\bar{T}}{m}\Delta t \tag{38}$$

because $E\left[\nu_k\right]=0$ and $E\left[\omega_k\right]=0$. The variance can be computed as

$$\sigma_{\Delta v}^2=E\left[(\Delta v-\overline{\Delta v})^2\right]=E\left[\left[\frac{\sigma}{m\beta}\sum_{k=0}^{n-1}(\alpha\nu_k+\gamma\omega_k)\right]^2\right] \tag{39}$$

Expanding the square of the sum yields

$$\begin{aligned}
\sigma_{\Delta v}^2=\frac{\sigma^2}{m^2\beta^2}E\Bigg[\sum_{k=0}^{n-1}\Bigg[&\alpha^2\nu_k^2+\gamma^2\omega_k^2\\
&+2\sum_{j<k}(\alpha\nu_k+\gamma\omega_k)(\alpha\nu_j+\gamma\omega_j)\Bigg]\Bigg]
\end{aligned} \tag{40}$$

As $E\left[\nu_k^2\right]=1$ and $E\left[\omega_k^2\right]=\sigma_\omega^2$, we recall that α and γ are constants.

$$\begin{aligned}
\sigma_{\Delta v}^2=\frac{\sigma^2}{m^2\beta^2}\Bigg[n(\alpha^2+\sigma_\omega^2\gamma^2)+2E\Bigg[\sum_{k=0}^{n-1}\Big(\sum_{j<k}&\alpha^2\nu_k\nu_j\\
&+\alpha\gamma\nu_k\omega_j+\alpha\gamma\nu_j\omega_k+\gamma^2\omega_k\omega_j\Big)\Bigg]\Bigg]
\end{aligned} \tag{41}$$

The last two terms are simplified. In fact, $E\left[\nu_j\omega_k\right]=0$ because future white noise cannot influence the current-time Gauss–Markov process, and $E\left[\omega_k\omega_j\right]=0$ because ω is white noise. Moreover, by applying Eq. (20) and exploiting $j<k$, we obtain

$$E\left[\nu_k\nu_j\right]=\mathrm{e}^{-\beta(k-j)\delta t} \tag{42}$$

$$E\left[\nu_k\omega_j\right]=\sigma_\omega^2\sqrt{\frac{1}{2\beta}(1-\mathrm{e}^{-2\beta\delta t})}\mathrm{e}^{-\beta(k-j-1)\delta t} \tag{43}$$

In conclusion,

$$\begin{aligned}
\sigma_{\Delta v}^2=\frac{\sigma^2}{m^2\beta^2}\Bigg\{n(\alpha^2+\sigma_\omega^2\gamma^2)+2\Bigg[&\alpha^2\sum_{k=0}^{n-1}\sum_{j<k}\mathrm{e}^{-\beta(k-j)\delta t}\\
&+\alpha\gamma\sigma_\omega^2\sum_{k=0}^{n-1}\sum_{j<k}\sqrt{\frac{1}{2\beta}(1-\mathrm{e}^{-2\beta\delta t})}\mathrm{e}^{-\beta(k-j-1)\delta t}\Bigg]\Bigg\}
\end{aligned} \tag{44}$$

Considering $\sigma_\omega=\sqrt{2\beta}$ and consequentially defining $\zeta=\sqrt{2\beta(1-\mathrm{e}^{-2\beta\delta t})}$, Eq. (44) can be further simplified as

$$\begin{aligned}
\sigma_{\Delta v}^2=\frac{\sigma^2}{m^2\beta^2}\Bigg[n(\alpha^2+2\beta\gamma^2)+2\Bigg(&\alpha^2\sum_{k=1}^{n-1}k\mathrm{e}^{-\beta(n-k)\delta t}\\
&+\alpha\gamma\zeta\sum_{k=1}^{n-1}k\mathrm{e}^{-\beta(n-k-1)\delta t}\Bigg)\Bigg]
\end{aligned} \tag{45}$$

A generalized geometrical series of the common coefficient e can be solved as

$$\sum_{k=1}^{n-1}k\mathrm{e}^k=\frac{\mathrm{e}-n\mathrm{e}^n+(n-1)\mathrm{e}^{n+1}}{(1-\mathrm{e})^2} \tag{46}$$

Eventually, Eq. (45) can be rewritten as Eq. (47):

$$\sigma_{\Delta v}^2=\frac{\sigma^2}{m^2\beta^2}[n(\alpha^2+2\beta\gamma^2)+2(\alpha^2\varsigma_1+\alpha\gamma\zeta\varsigma_2)] \tag{47}$$

where

$$\varsigma_1 = \sum_{k=1}^{n-1} k\mathrm{e}^{-\beta(n-k)\delta t} = \frac{(n-1)\mathrm{e}^{\beta\delta t} + \mathrm{e}^{-\beta(n-1)\delta t} - n}{(1-\mathrm{e}^{\beta\delta t})^2} \tag{48}$$

and

$$\begin{aligned}\varsigma_2 &= \sum_{k=1}^{n-1} k\mathrm{e}^{-\beta(n-k-1)\delta t} \\ &= \frac{(n-1)\mathrm{e}^{2\beta\delta t} - n\mathrm{e}^{\beta\delta t} + \mathrm{e}^{-\beta(n-2)\delta t}}{(1-\mathrm{e}^{\beta\delta t})^2}\end{aligned} \tag{49}$$

Consistent with the case of continuous driving noise, we assume that $\tau \gg \delta t$ (alternatively, $\beta\delta t \approx 0$). Thus, Eq. (47) can be simplified as

$$\sigma_{\Delta v}^2 = \frac{\sigma^2}{m^2\beta^2}\beta^2(n\delta t)^2 = \frac{\sigma^2}{m^2}\Delta t^2 \tag{50}$$

We recall that $n\delta t = \Delta t$ by definition. Under this assumption, the model consistency is maintained as expected because at the limit, the standard deviation is the same in the case of both the driving noises (Eq. (34)) and the driving sequence (Eq. (50)).

Typically, Δv statistics are expressed in relative terms with respect to the maneuver nominal value to obtain a result that does not depend on the maneuver magnitude and duration. In this case, the relative standard deviation can be computed. In the limit case, it is expressed as

$$\sigma_{\%} = \frac{\sigma_{\Delta v}}{\overline{\Delta v}} = \frac{\sigma}{\overline{T}} \tag{51}$$

4.2 Gauss–Markov process derivative

The Gauss–Markov process derivative can also be of interest for mission analysis applications.

By defining d as a generic variable representing a Gauss–Markov process derivative, it can be expressed as

$$d = \dot{\eta} = \frac{\mathrm{d}}{\mathrm{d}t}(\sigma\nu + \mu) = \sigma\dot{\nu} \tag{52}$$

where the model in Eq. (26) is used.

4.2.1 Continuous driving noise

Assuming a (theoretically) continuous driving noise, the Langevin equation in Eq. (1) still holds. Thus, Eq. (52) becomes

$$d = \sigma(-\beta\nu + \omega) \tag{53}$$

By exploiting the properties of the standard process, the mean is

$$\bar{d} = E[d] = 0 \tag{54}$$

The variance can be computed as

$$\begin{aligned}\sigma_d^2 &= E\left[(d-\bar{d})^2\right] = \sigma^2(\beta^2 E\left[\nu^2\right] + E\left[\omega^2\right]) - \bar{d}^2 \\ &= \sigma^2(\beta^2 + \sigma_\omega^2)\end{aligned} \tag{55}$$

Assuming that $\sigma_\omega = \sqrt{2\beta}$, the derivative variance is defined as

$$\sigma_d^2 = \sigma^2(\beta^2 + 2\beta) \tag{56}$$

4.2.2 Discrete driving sequence

Considering a driving sequence under the solution-preserving model as described in Section 3.2.1, the derivative of the standard random process can be computed using Eq. (13):

$$\dot{\nu}(t) = -\beta\nu + \omega_n \tag{57}$$

The use of the solution-preserving model avoids the non-derivable point in $t = t_n$, which is present in the statistics-preserving model.

As expected, the mean was

$$\bar{d} = \sigma E[\dot{\nu}] = 0 \tag{58}$$

where $\dot{\nu}$ is the sum of the zero-mean Gaussian. The variance can be computed as

$$\begin{aligned}\sigma_d^2 &= E\left[(d-\bar{d})^2\right] = \sigma^2 E\left[\dot{\nu}(t)^2\right] \\ &= \sigma^2(\beta^2 E\left[\nu^2\right] + E\left[\omega_n^2\right] - \beta E\left[\nu\omega_n\right])\end{aligned} \tag{59}$$

Taking into account Eq. (13), Eq. (59) can be reduced to

$$\sigma_d^2 = \sigma^2\left(\beta^2 + \sigma_\omega^2\mathrm{e}^{-\beta(t-t_n)}\right) \tag{60}$$

Because σ_ω is generally dependent on time, the variance of the derivative varies within each subinterval. Asymptotically, the variance in the derivative is

$$\sigma_d^2 = \sigma^2\left(\beta^2 + \frac{2\beta}{\delta t}\right) \tag{61}$$

In the last case, the derivative differs from the continuous driving noise result because the second term is divided by $\sqrt{\delta t}$. This result was expected because the solution-preserving model is a direct extension of the Euler–Maruyama scheme. Because of this inconsistency, extra care should be taken in the simulations when handling a Gauss–Markov process derivative. A simple mitigation action could be to use a characteristic sequence time equal to the time unit, although this can considerably increase the computational burden.

5 Results

A summary of the results on the noise characteristics for the Gauss–Markov processes is presented in Table 1, whereas Table 2 presents a review of the Gauss–Markov derived quantities.

Table 1 Summary of Gauss–Markov process noise characteristics

	Analytic solution	Simplified solution
Continuous driving noise	$\sigma_\omega = \sqrt{2\beta}\sigma$	—
Solution-preserving model	$\sigma_\omega = \beta\sqrt{\frac{1-\mathrm{e}^{-2\beta(t-t_0)}}{(1-\mathrm{e}^{-\beta(t-t_n)})^2+\chi\mathrm{e}^{-2\beta(t-t_n)}}}\sigma$	$\sigma_\omega = \sqrt{\frac{2\beta}{\delta t}}\sigma$
Statistics-preserving model	$\sigma_\omega = \sqrt{2\beta}\sigma$	—

Table 2 Summary of Gauss–Markov derived quantities, characteristics

		Mean	Analytic variance	Asymptotic variance
$q = \sigma\nu + \mu$	—	μ	σ^2	—
$I = \int_0^{\Delta t} q\mathrm{d}t$	Continuous noise	$\mu\Delta t$	$\frac{2}{\beta}\left(\Delta t - \frac{1-\mathrm{e}^{-\beta\Delta t}}{\beta}\right)\sigma^2$	$\sigma^2\Delta t^2$
	Discrete sequence	$\mu\Delta t$	$\frac{\sigma^2}{\beta^2}[n(\alpha^2+2\beta\gamma^2)+2(\alpha^2\varsigma_1+\alpha\gamma\zeta\varsigma_2)]$	$\sigma^2\Delta t^2$
$d = \frac{\mathrm{d}q}{\mathrm{d}t}$	Continuous noise	0	$\sigma^2(\beta^2+2\beta)$	—
	Discrete sequence	0	$\sigma^2(\beta^2+\sigma_\omega^2\mathrm{e}^{-\beta(t-t_n)})$	$\sigma^2\left(\beta^2+\frac{2\beta}{\delta t}\right)$

5.1 Discrete sequence propagation

To verify the validity of the presented models, simulations were performed, and the results were compared against the predicted values. Figure 1 shows the same Gauss–Markov process computed through different models. Figure 1(a) represents the continuous noise solution, evaluated using the Euler–Maruyama algorithm with a discretization $\delta t = 10^{-3}\tau$, whereas Figs. 1(b) and 1(c) present the results of the solution- and statistics-preserving models together with the absolute error with the continuous noise solution, respectively. From these figures, it can be inferred that both discrete models yield similar results and are able to retrace the Euler–Maruyama solution with relatively low errors. A Monte Carlo simulation with 1000 samples was performed to assess the accuracy of the statistics. Figure 2 shows the evolution in time of the variance for the three models. In addition, from a stochastic perspective, discrete models provide accurate results, mirroring the expected values from the theory. The errors of both the single solution and variance are given by the approximation error introduced by the Euler–Maruyama integration scheme, rather than those of the proposed models. As shown in Fig. 4, the errors against the SRA1 method used by Rößler [15], a (2.0, 1.5)-order integration scheme, demonstrate that it is more accurate than the simple Euler–Maruyama scheme. It should be noted that the errors decreased according to the integration scheme order, confirming that the errors in Figs. 1 and 2 are related to the approximation errors in the integration method.

Moreover, the oscillation around the theoretical values of $\sigma^2 = 1$ is due to the limited size of the pool. Figure 3 shows the time evolution of variance for the solution-preserving model with a discretization $\delta t = 10^{-3}\tau$, computed using 10,000 samples. As expected, a larger number of samples reduces the variability of σ^2, which is closer to the unit value. Moreover, the 99%-confidence bounds, indicated by the shaded areas, always enclose the theoretical value.

It is of paramount importance to determine the maximum discretization time for which the numerical solution of a standard Gauss–Markov process can still provide correct statistics. Figure 5 shows the process variance as a function of the discretization time. The Euler–Maruyama scheme cannot correctly represent the process for high values of discretization time, that is, with $\delta t > 0.1\tau$. In fact, it is the Itô generalization of a forward Euler scheme, and thus, it is inaccurate for large integration steps. However, both discrete process models can maintain the statistics in the theoretical range, as they are built to satisfy this property. This is confirmed by Fig. 6, where the estimated variance together with the 99%-confidence bounds are shown. The statistics-preserving model and analytic solution-preserving model (blue solid line in Fig. 6(b)) can give the correct process statistics, regardless of the discretization choices. In contrast, the simplified solution-preserving model (green dashed line in Fig. 6(b)) fails to provide a good result for high values of δt, as expected, because in these cases simplification hypotheses are no longer valid.

5.2 Uncertain trajectory propagation

Although discrete models can provide sequences representative of the original continuous process from a

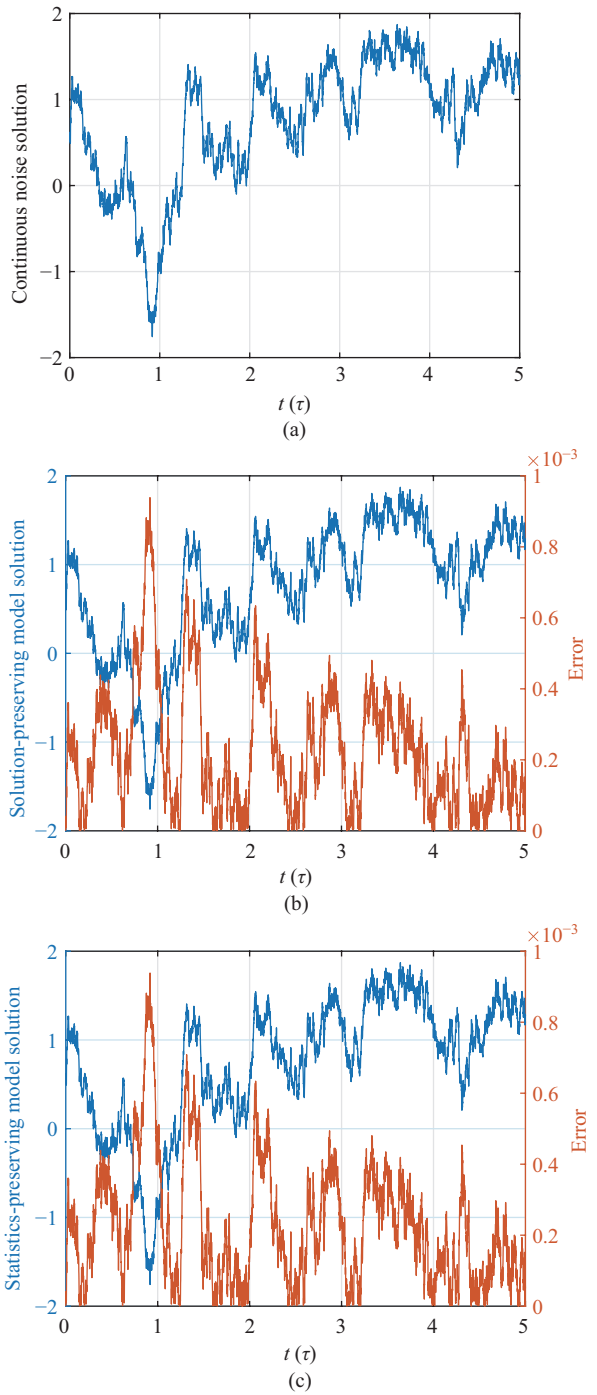

Fig. 1 Solution of the Langevin equation for the standard Gauss–Markov process, using (a) Euler–Maruyama scheme, (b) solution-preserving model, and (c) statistics-preserving model.

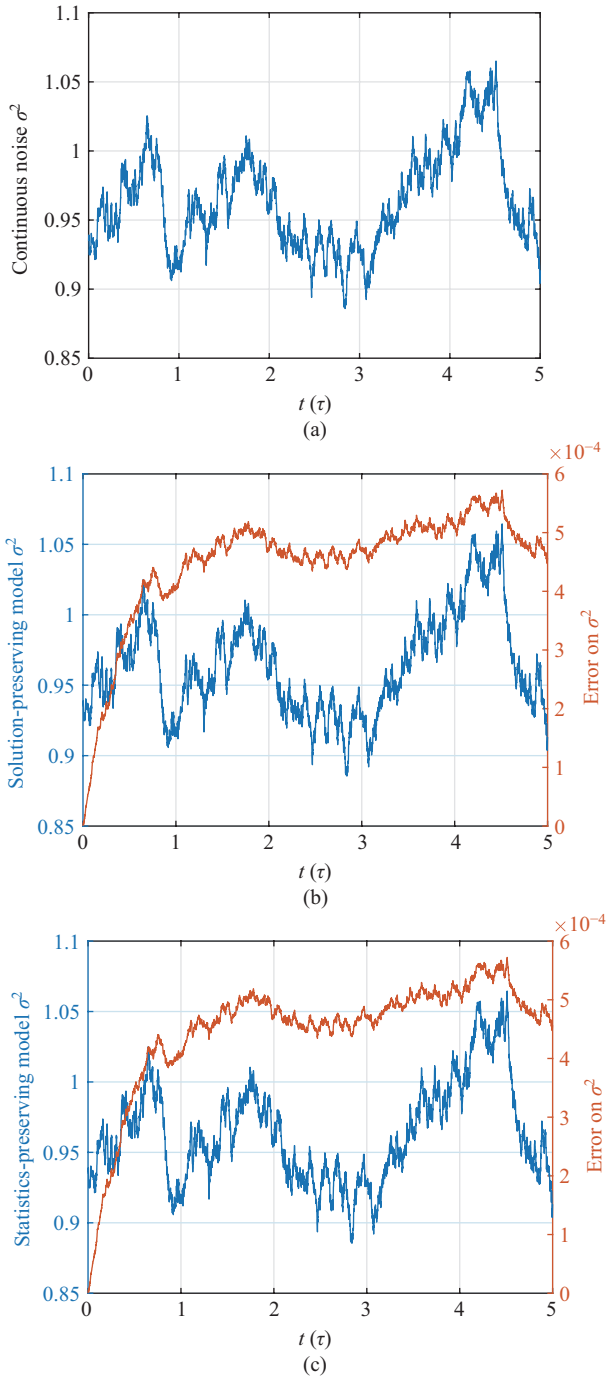

Fig. 2 Evolution in time of the standard Gauss–Markov process variance, computed with 10,000 samples, using (a) Euler–Maruyama scheme, (b) solution-preserving model, and (c) statistics-preserving model.

stochastic point of view, the impact of such discretization on a noisy trajectory should be assessed. Excessively tight discretization steps will yield results closer to the continuous case, but the computational burden can be unbearable. However, numerous steps can yield erroneous results.

A test-case scenario is built to evaluate the discretization time against the accuracy. The test case was a Hohmann transfer from the Earth to Mars, with the characteristics listed in Table 3. A simple test case was

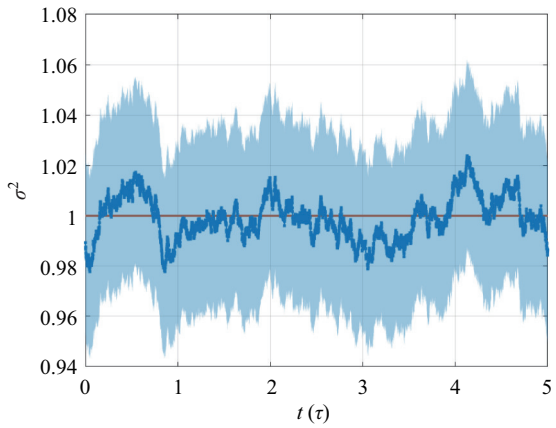

Fig. 3 Evolution in time of the standard Gauss–Markov process variance with $\delta t = 10^{-3}\tau$. The solid line is the theoretic value while the shaded area represents the 99%-confidence bounds of the variance.

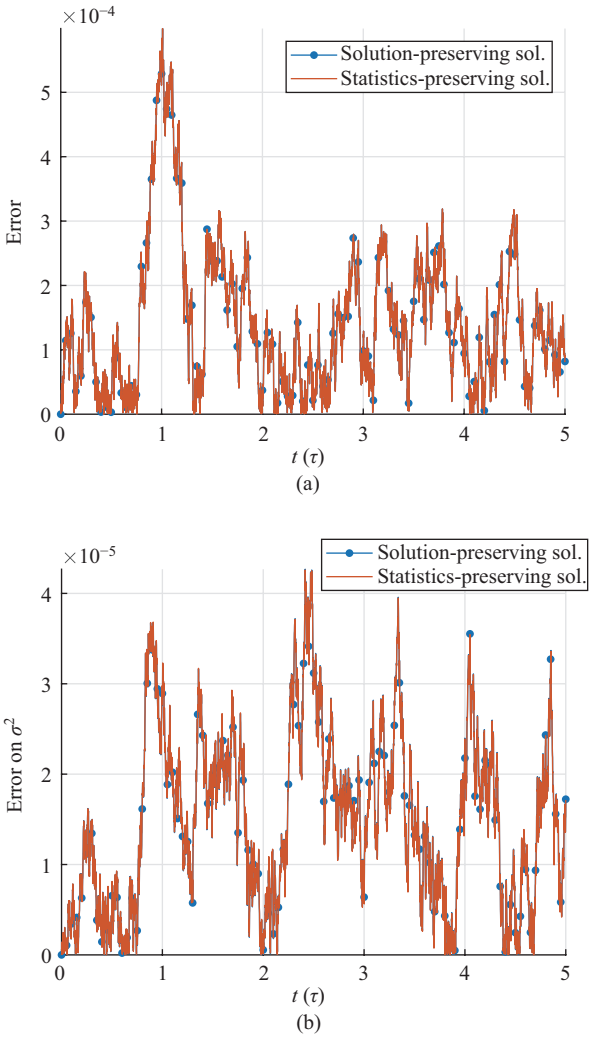

Fig. 4 Errors on the (a) solution and (b) variance of the solution- and statistics-preserving models against the SRA1 scheme for the standard Gauss–Markov process.

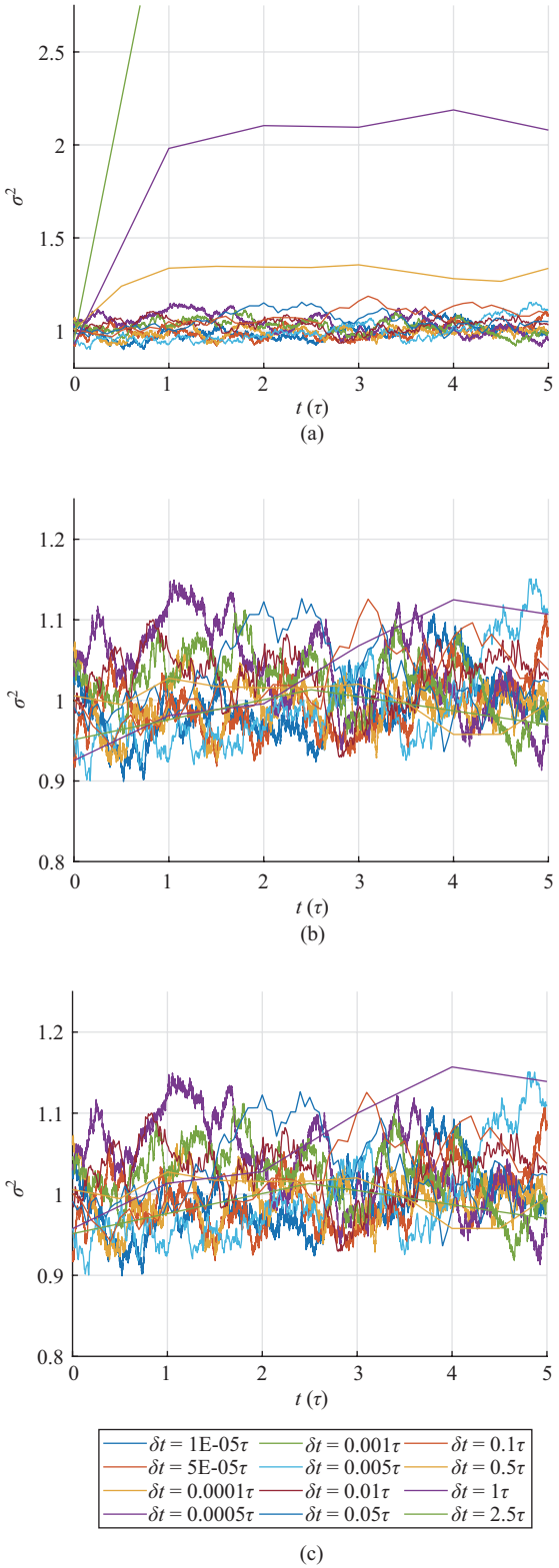

Fig. 5 Evolution in time of the standard Gauss–Markov process variance, computed with 1000 samples, for different discretization time δt, with (a) Euler–Maruyama scheme, (b) solution-preserving model, and (c) statistics-preserving model.

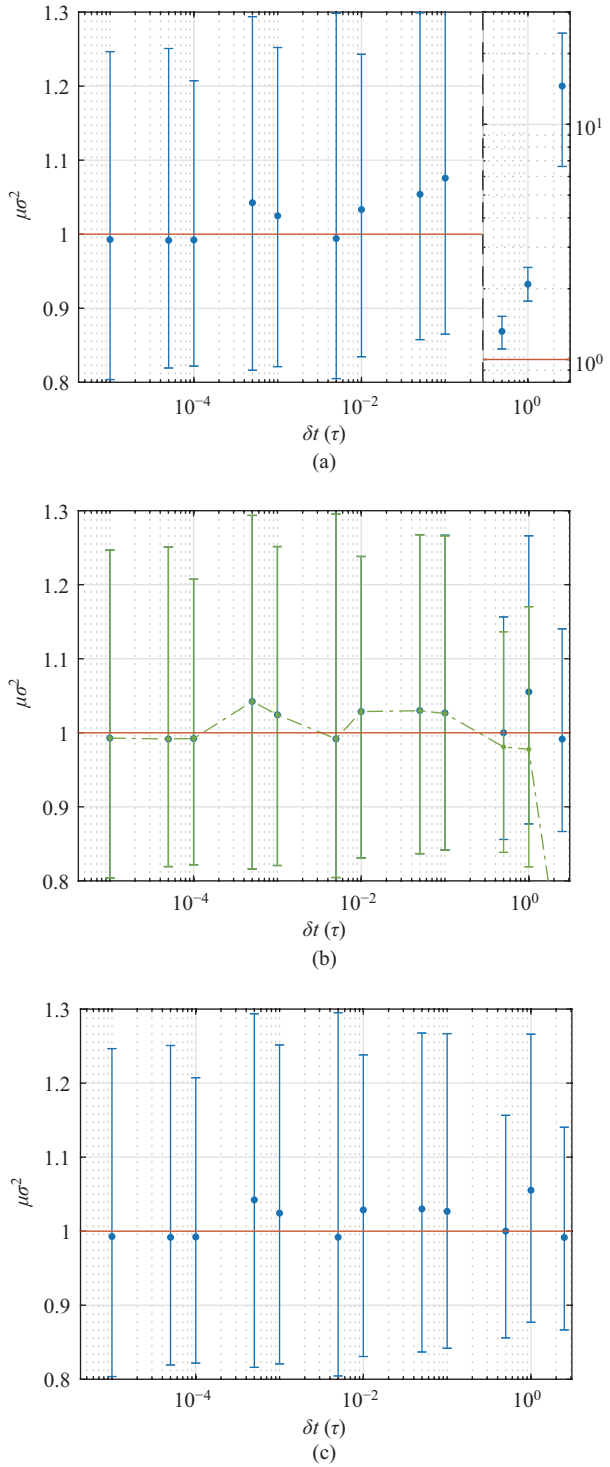

Fig. 6 Estimated value and confidence bounds for the standard Gauss–Markov process variance, computed with 1000 samples, for different discretization time δt, with (a) Euler–Maruyama scheme, (b) solution-preserving model, and (c) statistics-preserving model. In (b), the green dashed line represents the results for the simplified solution, whereas the blue line shows the results of the analytic one.

Table 3 Summary of test-case scenario trajectories

μ (km^3/s^2)	r_p (AU)	r_a (AU)	ToF (d)	σ (km/s^2)	β (1/d)
1.327×10^{11}	1	1.52	258.31	10^{-8}	1

selected to minimize the influence of chaotic dynamical behavior, integration errors, and numerical issues. Thus, any observed differences in dispersion can be confidently attributed to differences in the process discretization. In this case, the spacecraft dynamics are

$$\begin{cases} \dot{\boldsymbol{r}} = \boldsymbol{v} \\ \dot{\boldsymbol{v}} = -\frac{\mu}{\|\boldsymbol{r}\|^3}\boldsymbol{r} + \sigma\boldsymbol{\nu} \end{cases} \tag{62}$$

where $\boldsymbol{\nu}$ is a three-dimensional standard Gauss–Markov process with each dimension independent of the others. This multidimensional ECRV was used to represent all possible unmodeled accelerations.

The application of the Euler–Maruyama scheme or even the SDE higher-order schemes is not suitable in this case because it requires an extremely small step to correctly integrate the deterministic part. Therefore, the benchmark was obtained using a statistics-preserving model (Eq. (20)) with a discretization time of $\delta t = 10$ s. The solution was integrated using the Runge–Kutta 8(7) scheme. To correctly capture the effects of uncertainties, a maximum integration step of $\delta t/10$ was enforced.

Figure 7 shows the statistics of the test case trajectory with different discretization time, computed through a Monte Carlo simulation using 10,000 samples. Although the mean is always correctly retrieved, the standard deviation results strongly depend on the discretization step. In this case, for $\delta t \leqslant 10^4$ s $\approx 0.1\tau$, the standard deviation of the relative error is approximately 10^{-2}, which is within the accuracy of 10,000 samples. A two-way Kolmogorov–Smirnov test was used to test this claim. For larger δt, greater diffusion can be observed, leading to unrealistically large dispersions. This result was expected. A higher δt implies that the stochastic acceleration is kept constant in that direction for a longer time, leading to large deviations from the unperturbed case.

In conclusion, the models discussed in Section 3.2 can build discrete sequences with the desired stochastic characteristics regardless of the discretization time. However, special care on the δt selection should be taken when these sequences are used to model stochastic perturbations to avoid over-conservative and unrealistic behaviors in uncertainty quantification.

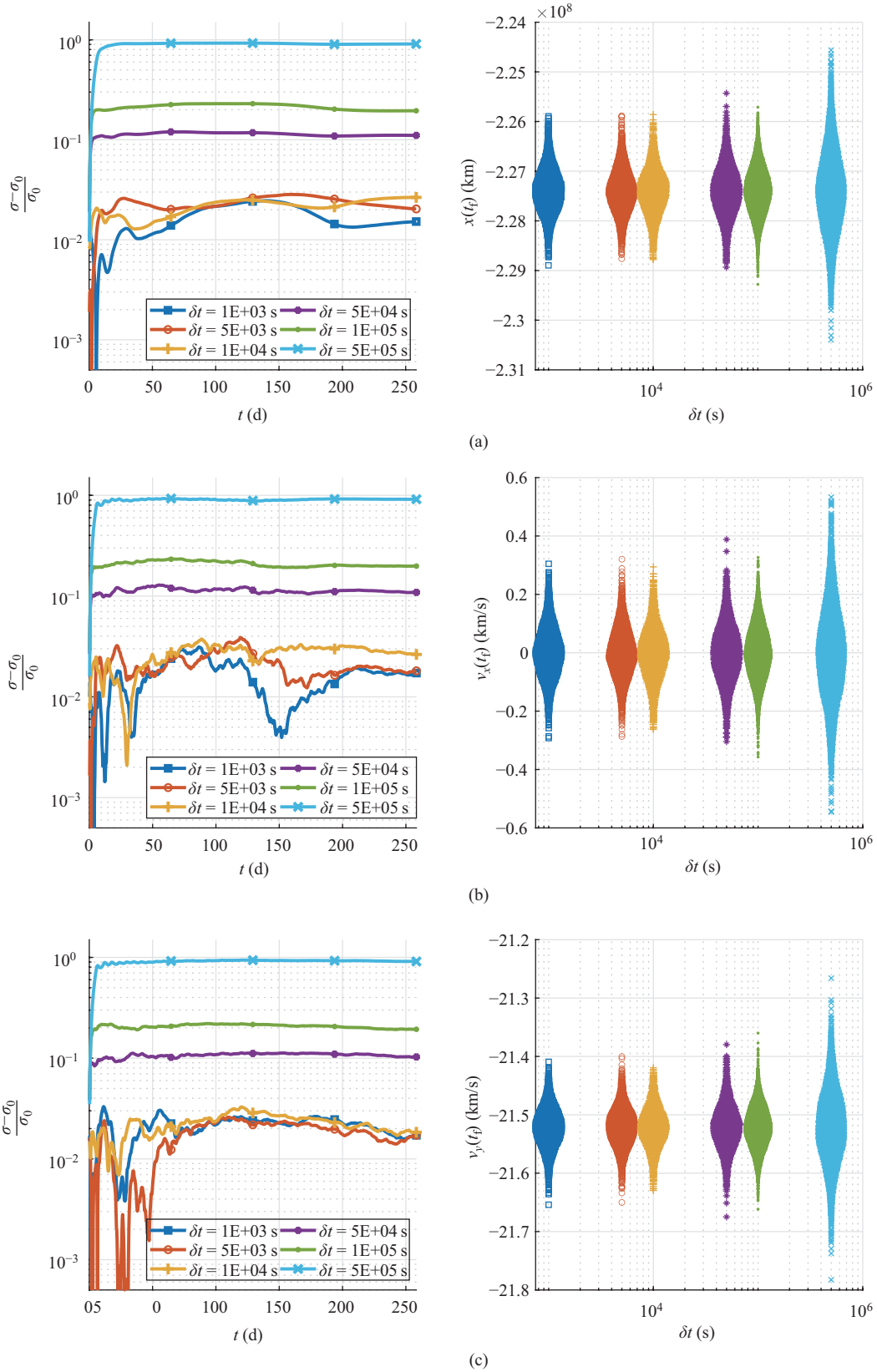

Fig. 7 Standard deviation relative error with respect to the benchmark solution σ_0 (left) and scatter chart at the final time (right) for different discretization time δt, for (a) x-, (b) v_x-, and (c) v_y-component of the state.

6 Conclusions

In this study, Gauss–Markov processes for mission analysis were characterized. After a general overview of the continuous Gauss–Markov process, two different models, one preserving the form of the solution and the other preserving the statistics, were introduced for a discrete computationally compatible version. Statistics associated with some derived quantities that could be of interest in the mission analysis were retrieved for both continuous and discrete cases, as well as the definition of a standard Gauss–Markov process. Under some hypotheses, the compatibility of the statistics between the two cases has been demonstrated for the integral of a process, whereas particular care should be taken in the case of the derivative. In conclusion, the discrete models were validated, and it was shown that they can provide a sequence with prescribed statistics, regardless of the discretization time. However, a low discretization time must be used when Gauss–Markov sequences are exploited as noisy accelerations because high discretization time can lead to an overestimation of the statistics associated with a given trajectory.

Funding note

Open access funding provided by Politecnico di Milano within the CRUI-CARE Agreement.

Acknowledgements

This project received funding from the European Research Council (ERC) under the European Union's Horizon 2020 Research and Innovation Program (Grant No. 864697).

Declaration of competing interest

The authors have no competing interests to declare that are relevant to the content of this article.

References

[1] Fehse, W. *Automated Rendezvous and Docking of Spacecraft*. Cambridge, UK: Cambridge University Press, **2003**.

[2] Luo, Y., Yang, Z. A review of uncertainty propagation in orbital mechanics. *Progress in Aerospace Sciences*, **2017**, 89: 23–39.

[3] Dei Tos, D. A., Rasotto, M., Renk, F., Topputo, F. LISA pathfinder mission extension: A feasibility analysis. *Advances in Space Research*, **2019**, 63(12): 3863–3883.

[4] Bottiglieri, C., Piccolo, F., Giordano, C., Ferrari, F., Topputo, F. Applied trajectory design for CubeSat close-proximity operations around asteroids: The Milani case. *Aerospace*, **2023**, 10(5): 464.

[5] Schutz, B., Tapley, B., Born, G. H. *Statistical Orbit Determination*. Elsevier, **2004**.

[6] Crassidis, J. L., Junkins, J. L. *Optimal Estimation of Dynamic Systems*. Chapman & Hall/CRC, **2004**.

[7] Lucor, D., Su, C. H., Karniadakis, G. E. Generalized polynomial chaos and random oscillators. *International Journal for Numerical Methods in Engineering*, **2004**, 60(3): 571–596.

[8] Uhlenbeck, G. E., Ornstein, L. S. On the theory of the Brownian motion. *Physical Review*, **1930**, 36(5): 823–841.

[9] Lawler, G. F. *Introduction to Stochastic Processes*. CRC Press, **2018**.

[10] Coddington, E. A. *An Introduction to Ordinary Differential Equations*. Toronto: General Publishing Company Ltd., **1961**.

[11] Vasicek, O. An equilibrium characterization of the term structure. *Journal of Financial Economics*, **1977**, 5(2): 177–188.

[12] Maybeck, P. S. *Stochastic Models, Estimation, and Control*. Cambridge, USA: Academic Press, **1982**.

[13] Kloeden, P. E., Platen, E. *Numerical Solution of Stochastic Differential Equations*. Springer Berlin, Heidelberg, **1992**.

[14] Deserno, M. How to generate exponentially correlated Gaussian random numbers. Department of Chemistry and Biochemistry UCLA, USA, **2002**. Available at https://www.cmu.edu/biolphys/deserno/pdf/corr_gaussian_random.pdf.

[15] Rößler, A. Runge–Kutta methods for the strong approximation of solutions of stochastic differential equations. *SIAM Journal on Numerical Analysis*, **2010**, 48(3): 922–952.

Carmine Giordano holds a Ph.D. degree in aerospace engineering from Politecnico di Milano, Italy. Currently, he is a postdoc researcher within the ERC project EXTREMA. His main fields of interest are nonlinear astrodynamics and trajectory optimization. He participated in three CubeSat mission Phases A funded by ESA (LUMIO, M-ARGO, and Hera's Milani) as a mission analyst. E-mail: carmine.giordano@polimi.it